Thermo X

https://doi.org/10.70401/tx.2026.0030

Supplementary information

Nonmonotonic phonon thermal transport during layer-by-layer magnetic switching in four-layer CrSBr

Rongkun Chen, Yan Luo, Junhan Li, Weina Ren, Shiqian Hu

Table S1. Relative energies and estimated equivalent magnetic field.

Name	Relative energy, $\Delta E = E - E_{\mathrm{AFM}}$ (meV)	equivalent magnetic field (*T*)	Experiment magnetic field (*T*)
AFM	0.00	0	0
FiM1	0.49	~0.18	~0.12
FiM2	1.13	~0.27	~0.22
FM	2.54	~0.45	~0.4

Table. S2. Magnetic space groups and Γ-point phonon symmetry for the four collinear magnetic configurations. The relevant antiunitary operations square to +1 at *Γ* for spinless phonons; hence, no Kramers-like twofold degeneracy is enforced.

Name	Crystallographic Space Group	Magnetic Space Group	Magnetic point group	Unitary operations	Antiunitary operations	-point single-valued irreps
AFM	*Pmmn*, No. 59	*Pm'mn*, 59.407	*m'mm*	4	4	1D
FiM1	*Pmmn*, No. 59	*Pm'm2'*, 25.59	*m'm2'*	2	2	1D
FiM2	*Pmmn*, No. 59	*Pm'm2'*, 25.59	*m'm2'*	2	2	1D
FM	*Pmmn*, No. 59	*Pm'mn*, 59.410	*m'm'm*	4	4	1D

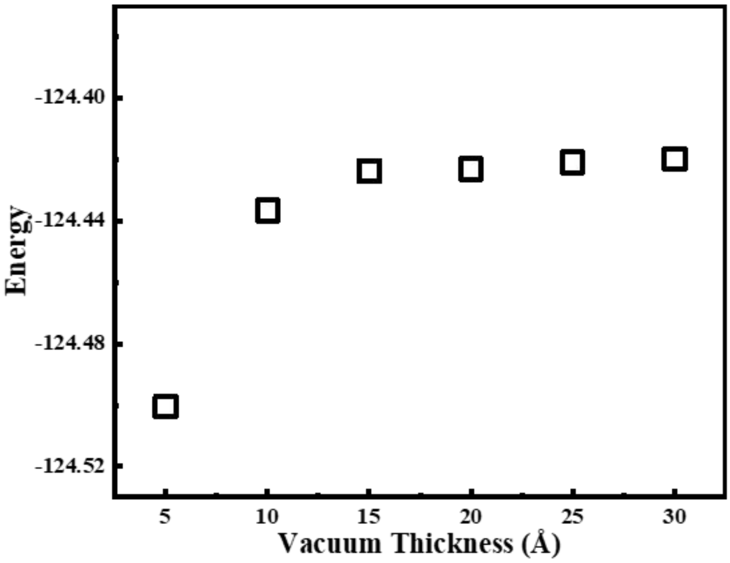

Figure S1. Vacuum-thickness convergence test for the antiferromagnetic (AFM) configuration. Total energy as a function of vacuum spacing (5-30 Å). The energy is well converged when the vacuum thickness exceeds 15 Å.

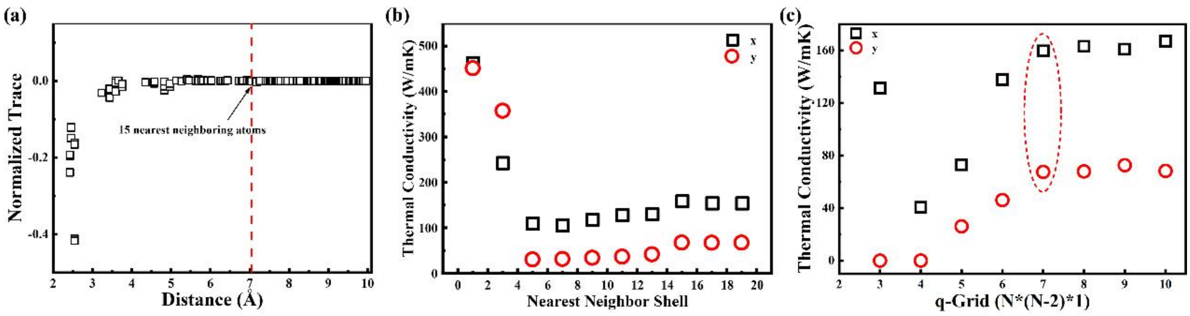

Figure S2. Convergence tests for the normalized trace of force constants, third-order IFC cutoff and lattice thermal conductivity with respect to grid density. (a) Normalized trace of the second-order force constant matrix, which converges to nearly zero beyond 6 Å; considering interactions up to 15 nearest-neighbor atoms for the third-order force constants already yields a well-converged result; (b) Calculated at the adopted 7 × 5 × 1 PBTE q-point mesh. The thermal conductivity reaches a well-converged plateau when interactions up to the 15th nearest-neighbor shell are included; (c) Convergence of the lattice thermal conductivity with respect to grid density in solving the phonon Boltzmann transport equation; a grid density of 7 × 5 × 1 is sufficient to achieve good convergence.

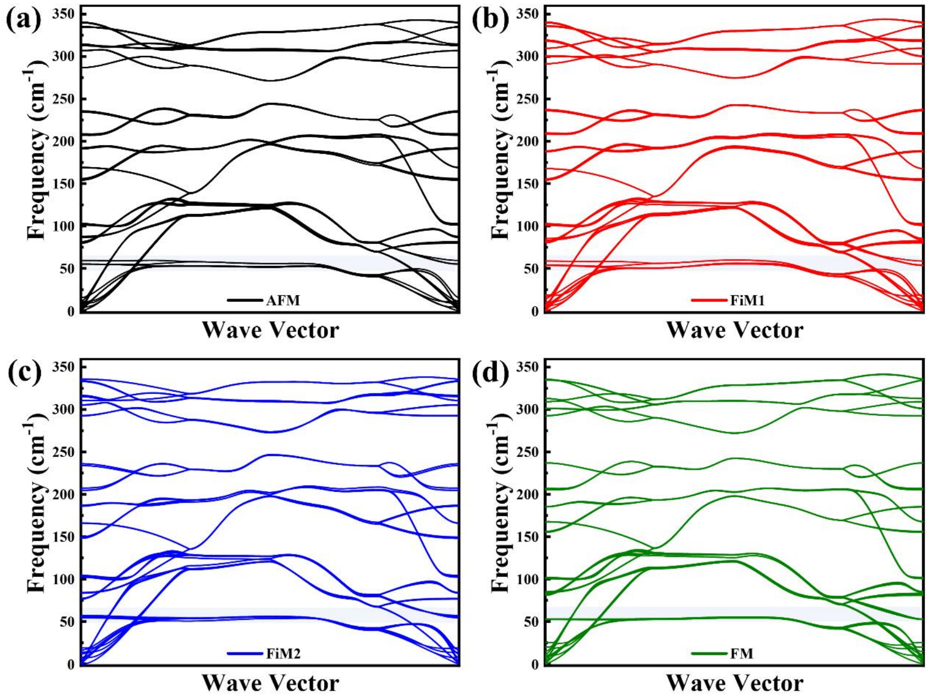

Figure S3. Phonon dispersion relations. (a)-(c) show the phonon dispersion relations of four-layer CrSBr under successive layer-by-layer flipping. The dispersion relations in the light blue regions exhibit degeneracy changes during the flipping process.

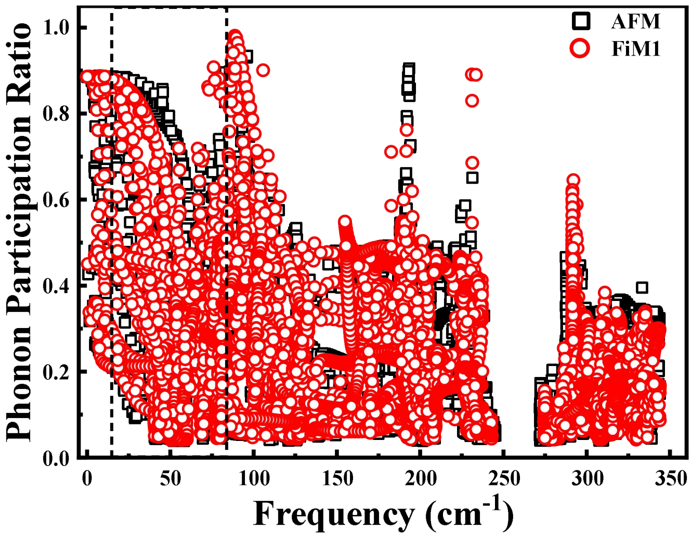

Figure S4. Phonon participation ratio. Phonon participation ratio (PR) as a function of frequency. Most phonon modes exhibit PR values below 0.4, indicating relatively localized vibrational characteristics. Compared with other magnetic states, the FiM1 configuration (red circles) shows noticeably reduced PR values in the 20-80 cm^{-1} frequency range.

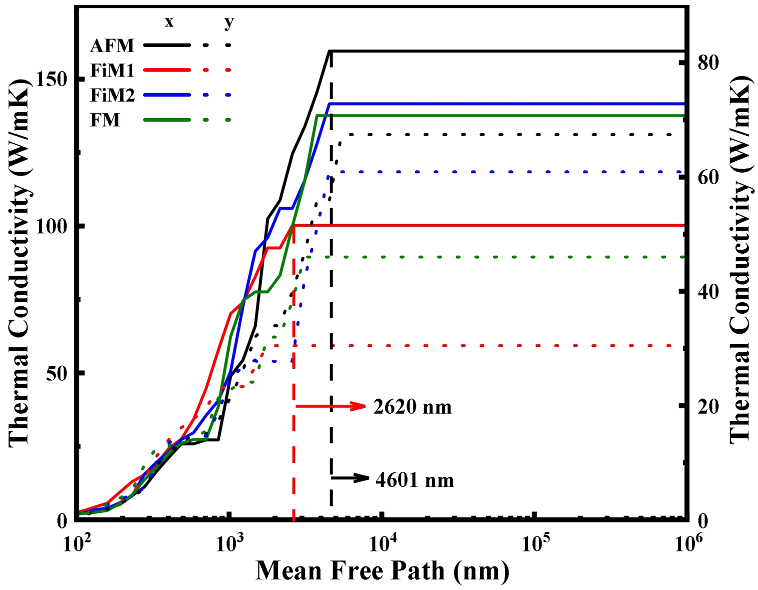

Figure S5. Cumulative lattice thermal conductivity as a function of phonon mean free path (MFP). The dominant contribution arises from phonons with MFPs below approximately 4601 nm. Compared with the AFM state, the FiM1 configuration exhibits a clear shift toward shorter MFPs, consistent with enhanced low-frequency three-phonon scattering.

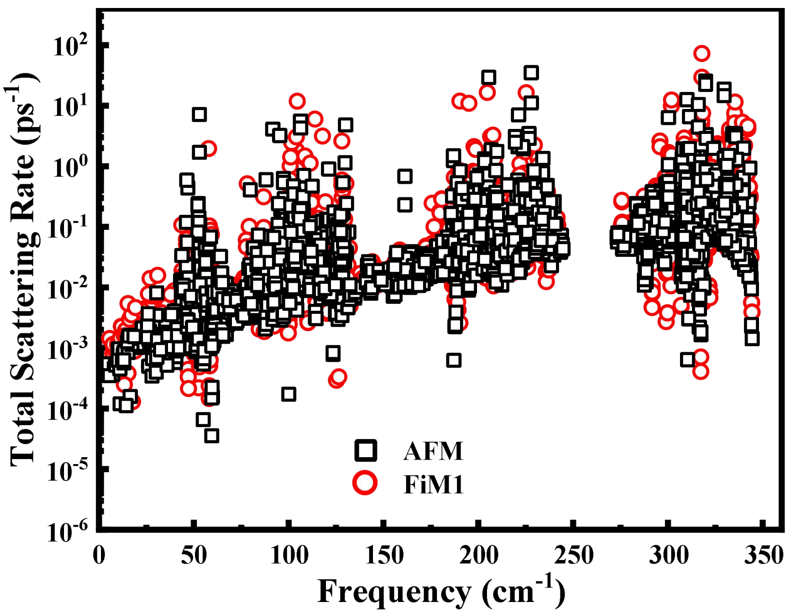

Figure S6. Three-phonon scattering rates. Total three-phonon scattering rates as a function of phonon frequency for different magnetic configurations. The FiM1 state (red circles) exhibits significantly enhanced scattering rates below 80 cm^{-1} compared with the AFM state (black squares).

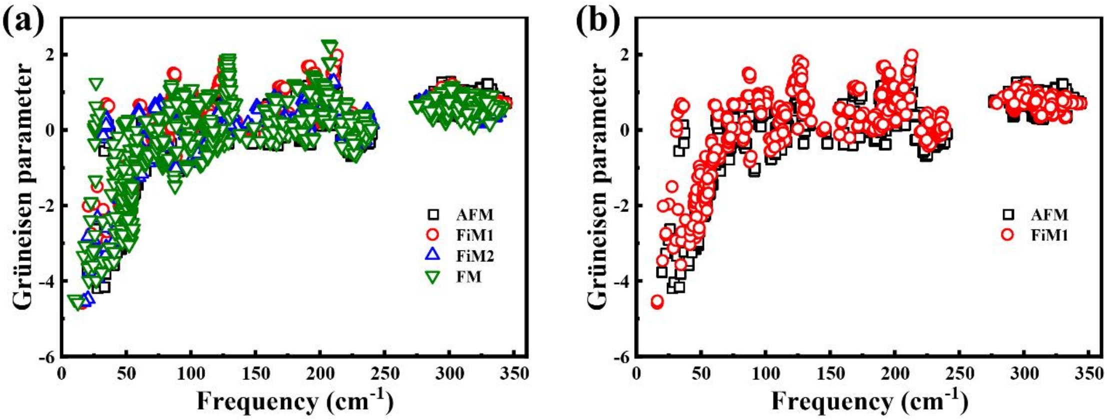

Figure S7. Grüneisen parameters for different magnetic configurations. The parameters are markedly enhanced in the FiM1 state, particularly for low-frequency modes below approximately 80 cm^{-1}, directly indicating stronger anharmonicity of the phonons that dominate heat transport.

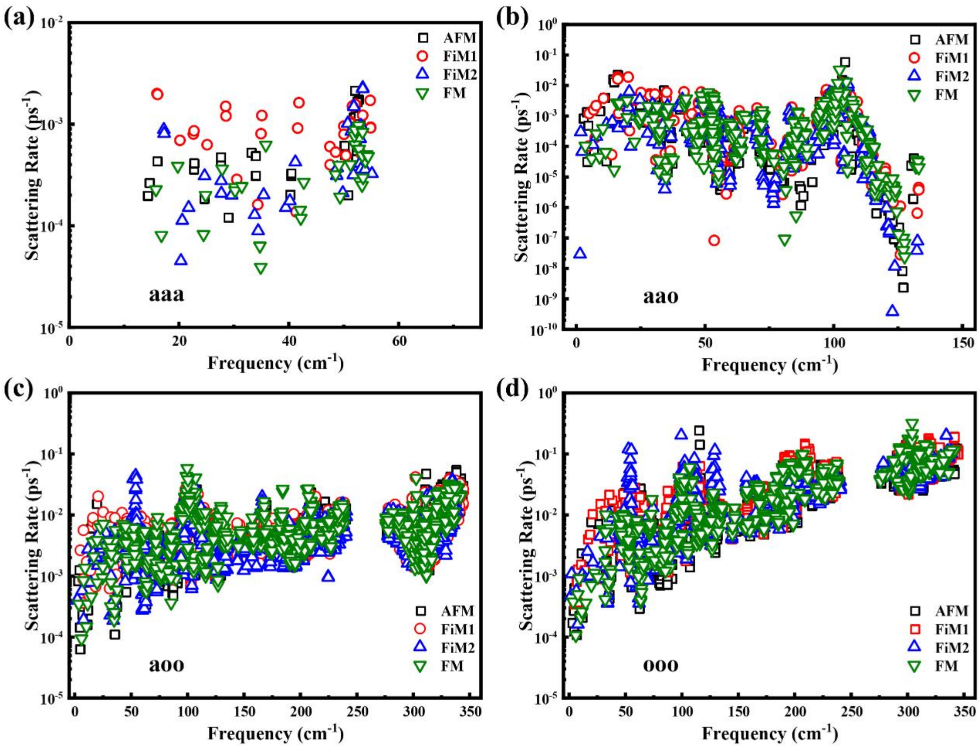

Figure S8. Scattering channels. The FiM1 state exhibits enhanced scattering in the low-frequency region across all channels, whereas the AFM, FiM2, and FM states display substantially weaker and mutually similar behavior. These findings provide quantitative support that the thermal-conductivity reduction in FiM1 originates primarily from enhanced anharmonic scattering rather than from changes in group velocity or from an expansion of the scattering phase space.